Energy Migration in a Poly(phenylene ethynylene): Determination of Interpolymer Transport in Anisotropic Langmuir−Blodgett Films

Igor A. Levitsky,[†] Jinsang Kim,[†,‡] and Timothy M. Swager*[,†]

Contribution from the Departments of Chemistry and of Materials Science and Engineering, Massachusetts Institute of Technology, Cambridge, Massachusetts 02139

Received July 23, 1998

Abstract: The photophysical and energy transport properties of a poly(*p*-ethynylene), **1**, were investigated in thin films. Highly aligned films of a precise thickness, prepared by sequential monolayer deposition using the Langmuir−Blodgett technique, were surface modified with luminescent traps (acridine orange, AO) for energy transfer studies. The degree of energy transfer to the traps was investigated as a function of the AO concentration and the number of polymer layers. An increased efficiency of energy transfer to the traps was observed with increasing numbers of layers until an approximate thickness of 16 layers. This behavior is consistent with a transition to a three-dimensional energy migration topology. A phenomenological model for the transport was proposed, and solutions were obtained by numerical methods. The model yields a fast ($>6 \times 10^{11}$ s^{-1}) rate of energy transfer between polymer layers and a diffusion length of more than 100 Å in the *Z* direction (normal to the film surface).

Introduction

Energy migration processes have been studied extensively in polymers that have saturated backbones and pendant chromophores.[1−4] In recent years, there has been growing interest in energy migration processes that occur in conjugated polymers, which can display both through-bond and through-space (Förster) transport mechanisms.[5−8] The poly(phenylene ethynylenes) have seen considerable interest due to their rigid geometry and ability to behave as efficient conduits for long-range energy transfer.[9−12] The capacity of these systems to display facile energy migration has been of particular interest to this laboratory for the amplification of fluorescence-based chemosensory signals.[10,13] Additional interest stems from the fact that energy transfer in supramolecular systems is a critical element in many artificial energy-harvesting schemes.[14] There is also substantial technological interest in energy migration since the electroluminescence from conjugated polymers is often dominated by radiative recombination at dilute low-energy-trapping sites. Similarly, the ability of minority defect sites to dominate a polymer's fluorescence has been used to detect dilute imperfections in complex conjugated ladder polymers.[15]

Although superficially poly(*p*-phenylene ethynylenes) would appear to have a rigid-rod structure, with high degrees of polymerization, these materials display a coiled solution structure with persistent lengths of approximately 15 nm.[16] For polymers isolated in dilute solution, the excitation's migration is a one-dimensional random-walk along the polymer's backbone. Considering the high efficiency of energy transfer in these systems[9−13] relative to systems with pendant chromophores,[1−4] the transport mechanism within a single polymer likely involves facile through-bond energy transfer processes. To realize the highest amplification potential of these polymers in our sensory

[†] Department of Chemistry.

[‡] Department of Materials Science and Engineering.

(1) Guillet, J. *Polymer Photophysics and Photochemistry: An Introduction to the Study of Photoprocesses in Macromolecules*; Cambridge University Press: Cambridge, U.K., 1987.

(2) (a) Byers, J. D.; Friedrich, M. S.; Friesner, R. A.; Webber, S. E. In *Molecular Dynamics in Restricted Geometries*; Klafter, J., Drake, J. M., Eds.; Wiley: New York, 1988; pp 99−144. (b) Kizerow, D. J.; Itoh, Y.; Webber, S. E. *Macromolecules* **1997**, *30*, 2934. (c) Levitsky, I. A.; Webber, S. E. *J. Lumin.* **1998**, *78*, 147.

(3) (a) Fox, R. B.; Price, T. R.; Cozzens, R. F.; Echols, W. H. *Macromolecules* **1974**, *7*, 937. (b) Fox, R. B.; Price, T. R.; Cozzens, R. F.; MacDonald, J. R. *J. Chem. Phys.* **1972**, *57*, 534.

(4) Winnik, M. A. *Photophysical and Photochemical Tools in Polymer Science*; Reidel: Dordrecht, Holland, 1986; pp 293−324.

(5) (a) Pakbaz, K.; Lee, C. H.; Hagler, T. W.; McBranch, D.; Heeger A. J. *Synth. Met.* **1994**, *64*, 295. (b) Patil, A. O.; Heeger. A. J.; Wudl, F. *Chem. Rev*. **1988**, *88*, 183.

(6) (a) Samuel, I. D. W.; Crystall, B.; Rumbles, G. P. L.; Holmes, A. B.; Friend, R. H. *Chem. Phys. Lett.* **1993**, *213*, 472. (b) Samuel, I. D. W.; Crystall, B.; Rumbles, G.; Burn, P. L.; Holmes, A. B.; Friend R. H. *Synth. Met.* **1993**, *54*, 281.

(7) (a) Bässler, H.; Deuben, M.; Huen, S.; Lemmer, U.; Mahrt, R. F. *Z. Phys. Chem.* **1994**, *184*, 233. (b) Huen, S.; Mahrt, R. F.; Greiner, A.; Lemmer, U.; Kersting, R.; Bässler, H.; Halliday, D. A.; Bradley, D. D. C.; Burn, P. L.; Holmes, A. B. *J. Phys.: Condens. Matter* **1993**, *5*, 247. (c) Mahrt, R. F.; Pauk, T.; Lemmer, U.; Siegner, U.; Hopmeier, M.; Hennig, R.; Bässler, H.; Gobel, E. O.; Kurz, H.; Wegmann, G.; Bolivar, P. H.; Scherf, U.; Müllen, K. *Phys. Rev. B* **1996**, *54*, 1759.

(8) (a) Rothberg, L. J.; Yan, M.; Papadimitrakopoulos, F.; Galvin, M. E.; Kwock, E. W. *Synth. Met*. **1996**, *80*, 41. (b) Yan, M.; Rothberg, L. J.; Papadimitrakopoulos, F.; Galvin, M. E.; Miller, T. M. *Phys. Rev. Lett.* **1994**, *73*, 744.

(9) Swager, T. M.; Gil, C. J.; Wrighton, M. S. *J. Phys. Chem.* **1995**, *99*, 4886.

(10) (a) Zhou, Q.; Swager, T. M. *J. Am. Chem. Soc.* **1995**, *117*, 7017. (b) Zhou, Q.; Swager, T. M. *J. Am. Chem. Soc.* **1995**, *117*, 12593. (c) Yang, J.-S.; Swager, T. M. *J. Am. Chem. Soc.* **1998**, *120*, 5321.

(11) Devadoss, C.; Bharathi, P.; Moore, J. S. *J. Am. Chem. Soc.* **1996**, *118*, 9635.

(12) Ley, K. D.; Whittle, C. E.; Bartberger, M. D.; Schanze, K. S. *J. Am. Chem. Soc.* **1997**, *119*, 3423.

(13) Other conjugated polymers have also be used for the development of new fluorescence chemosensors: (a) Wang, B.; Wasielewski, M. R. *J. Am. Chem. Soc.* **1997**, *119*, 12. (b) Kimura, M.; Horai, T.; Hanabusa, K.; Shirai, H. *Adv. Mater.* **1998**, *10*, 459. (c) Crawford, K. B.; Goldfinger, M. B.; Swager, T. M. *J. Am. Chem. Soc.* **1998**, *120*, 5187.

(14) (a) Meyer, T. J. *Acc. Chem. Res.* **1989**, *22*, 163. (b) Dupray, L. M.; Devenney, M.; Striplin, D. R.; Meyer, T. J. *J. Am. Chem. Soc.* **1997**, *119*, 10243.

(15) Goldfinger, M. B.; Swager, T. M. *J. Am. Chem. Soc.* **1994**, *116*, 7895.

(16) Cotts, P. M.; Swager, T. M.; Zhou, Q. *Macromolecules* **1996**, *29*, 7323.

10.1021/ja982610t CCC: $18.00
Published on Web 02/04/1999

schemes,[10] the excitations must sample the greatest possible number of polymer repeating units. In this case, the excitations will have the highest probability of encountering an occupied receptor. One-dimensional random-walks do not provide the optimal amplification because an excitation necessarily retraces portions of the polymer backbone multiple times. Hence, we are interested in conjugated polymer assemblies capable of supporting efficient two- and three-dimensional random-walks of the excitations. This increased dimensionality decreases the probability of an excitation retracing a given segment of the polymer and thereby produces larger amplification in sensory schemes. The efficiency of intermolecular energy migration depends on facile dipolar Förster-type processes, which are optimal when the transition dipoles of the donor and acceptor groups are aligned. As a consequence, films of aligned polymers with extended chain conformations provide an ideal situation for energy migration.

In this contribution, we report investigations of energy migration processes in highly aligned monolayer and multilayer films of poly(phenylene ethynylenes) prepared by the Langmuir−Blodgett (LB) deposition technique.[17] By using a luminescence traps located exclusively at the polymer surface, we have been able to determine the efficiency of energy migration in the direction normal to the surface. Equations describing this process, our experimental findings, and modeling by numerical methods have allowed the determination of the relative rates of energy migration in these systems. Moreover, our studies confirm that interlayer Förster-type energy migration processes are very fast and provide an important transport mechanism.

Results and Discussion

The LB deposition technique was used to produce highly anisotropic polymer films of **1**[17,18] with a well-defined thickness.

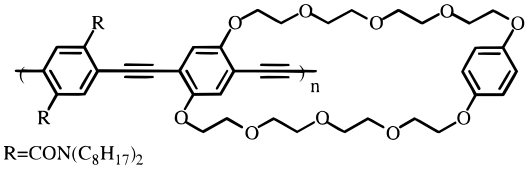

1

The film thickness increases linearly with the number of layers transferred,[17] thereby producing a well-defined geometry and distance for which to study energy migration processes. Additionally, the Langmuir−Blodgett technique creates films with spectroscopic properties different from those obtained from simple spin-casting. Most notable is the fact that the emissions from the Langmuir−Blodgett films more closely resemble those observed in solution (Figure 1). Both the LB films and the spin-cast films display a red shift relative to their solution spectra. However, in the case of the spin-cast films there is also a noticeable change in the emission shape. These spectral changes are most likely the result of interactions (π-stacking) between the polymer backbones.[19] Indeed, as shown in Figure 2, we observe a progression of red shifts in the LB film's emission with increasing numbers of layers, suggesting that π-stacking interactions become more prevalent in thicker films.

(17) Polymer **1** has been studied previously by our group.[10a,b] The details on the LB processing of this polymer will be reported soon: Kim, J.; McHugh, S. K.; Swager, T. M. *Macromolecules*. In press.

(18) For a review of the LB deposition of polymers, see: Wegner, G. *Thin Solid Films* **1992**, *216*, 105.

(19) Cornil, J.; dos Santos, D. A.; Crispin, X.; Silbey, R.; Brédas, J. L. *J. Am. Chem. Soc.* **1998**, *120*, 1289.

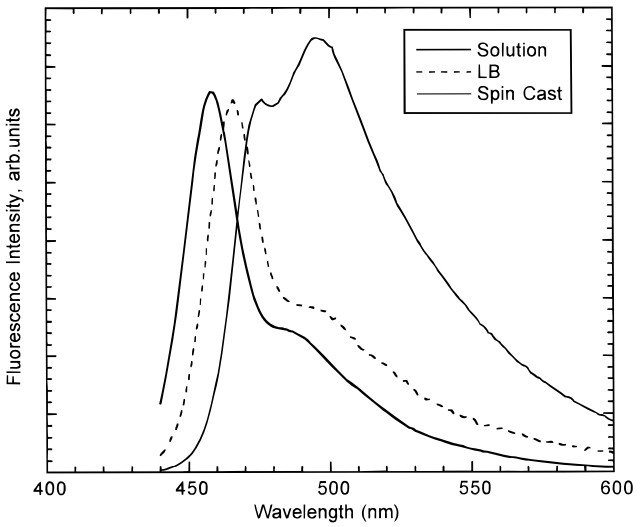

Figure 1. Comparison of the emission spectra (λ_{ex} = 420 nm) for **1** in solution, as a highly aligned LB film (2 layers), and as spin-cast from $CHCl_3$.

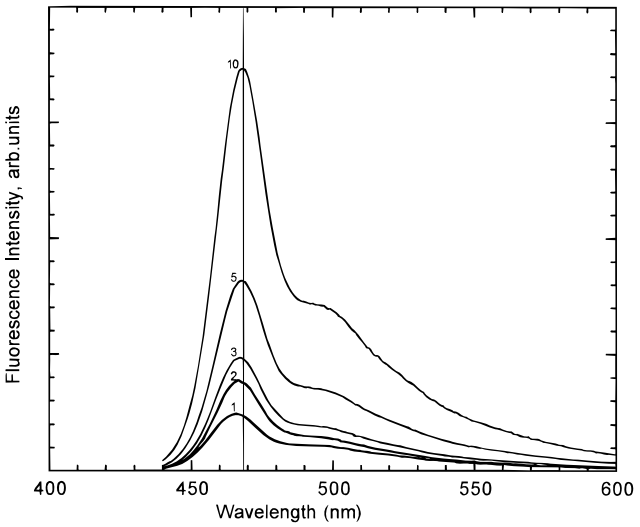

Figure 2. Emission spectra (λ_{ex} = 420 nm) for LB films of **1** containing 1, 2, 3, 5, and 10 aligned layers.

The lifetimes were determined by a phase detection method,[20] and the primary data and the experimental fits are shown in Figure 3. It should be noted that the solution lifetimes are in complete agreement with values previously determined using a pulsed excitation and correlated photon counting.[10b] Solutions of **1** exhibit a monoexponential decay and lifetime of 640 ps; however, as is typical for polymer solids,[1−8] both the LB and spin-cast films display non-monoexponential behavior. The emission decays of films are best described with biexponential functions with small components (≈1−3%) of a species that is much longer lived (1.2−1.8 ns) than the principal emission. Hence, in qualitative terms, the lifetimes, determined at the emission maxima (Figure 3a), can be considered the result of monoexponential fits with approximate values of 172 and 95 ps for LB and spin-cast films, respectively. The fact that energy migration is present can be readily seen in the wavelength-dependent lifetime measurements on spin-cast films (Figure 3b). These lifetime characteristics are consistent with the model of

(20) (a) Hieftje, G. M.; Vogelstein, E. E. In *Modern Fluorescence Spectroscopy*; Wehry, E. L., Ed.; Plenum Press: New York, 1981. (b) Lakowicz, J. R. *Principles of Fluorescence Spectroscopy*; Plenum Press: New York, 1986.

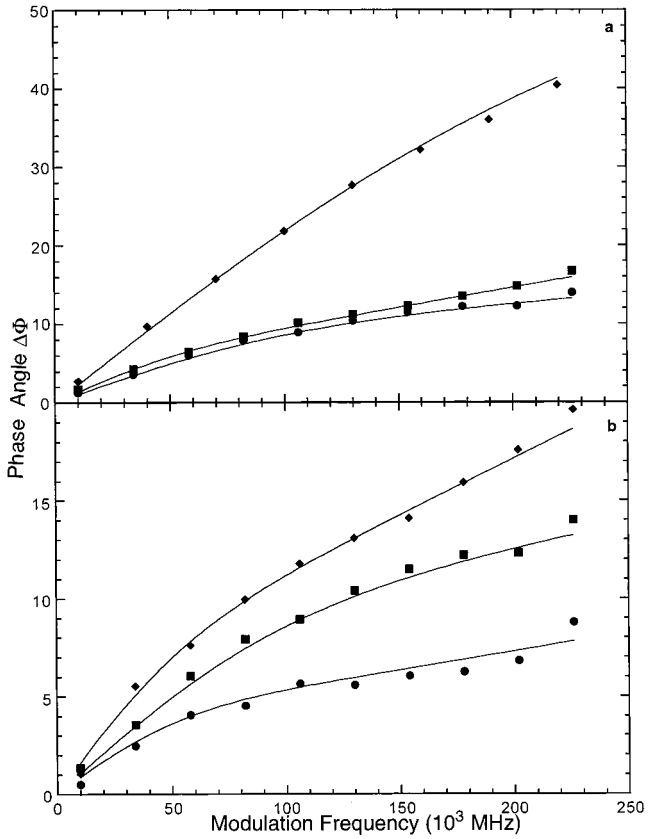

Figure 3. Experimental data points (λ_{ex} = 360 nm) and the mono- and biexponential fits (solid lines) for the reported lifetimes of **1** (see text for more details). (a) Key: ●, spin-cast film (λ_{det} = 475 nm); ■, 10-layer LB film (λ_{det} = 468 nm); ◆, solution film (λ_{det} = 458 nm). (b) Lifetimes of spin-cast films determined by monitoring signals at specific wavelengths: ●, λ_{det} = 460 nm; ■, λ_{det} = 475 nm; ◆, λ_{det} = 495 nm.

Bässler wherein the polymer is described as a continuous distribution (usually Gaussian) of site energies.[7] In this model, each state corresponds to a conjugated polymer segment that is interrupted by chain defects (conformational or chemical), with the longer segments having lower energy, and energy migration is described as incoherent hopping of excitations to lower energy states. Emission from high-energy states should exhibit a faster decay rate due to energy transfer to lower energy chromophores within the system. Correspondingly, as shown in Figure 3b, the lifetime increases (monoexponential fit, τ = 74, 95, and 200 ps) when monitored at progressively longer wavelengths (λ = 460, 475, and 495 nm, respectively). Unfortunately, similar wavelength studies could not be performed on LB films due to the lower fluorescence intensity of these samples.

The lifetime and spectral differences between the spin-cast and LB films are attributed to the high degree of alignment of the LB films and/or the differences in film thickness. It appears that the cyclophane moieties in an aligned sample more efficiently organize to block the π-stacking interactions responsible for self-quenching. In the case that polymer chains are randomly aligned, as is the case in spin-cast films, the polymer chains can fit in the clefts between the cyclophane moieties and thereby achieve greater π-stacking interactions. Chain alignment therefore has the ability to generate more highly luminescent solid-state conjugated polymer assemblies,[15] and this fact is of general importance for sensors in electroluminescence applications. The differences in the spin-cast and LB films could also be the result of film thickness effects.[21] In this case, the decrease in lifetime and increase in the efficiency of energy transfer to low-energy traps would be due to a three-dimensional topology in spin-cast films as compared to a two-dimensional topology in LB films. However, considering that LB films of **1** displayed only a minor shift in emission with increasing thickness (Figure 2), we believe any influences of this nature are relatively minor.

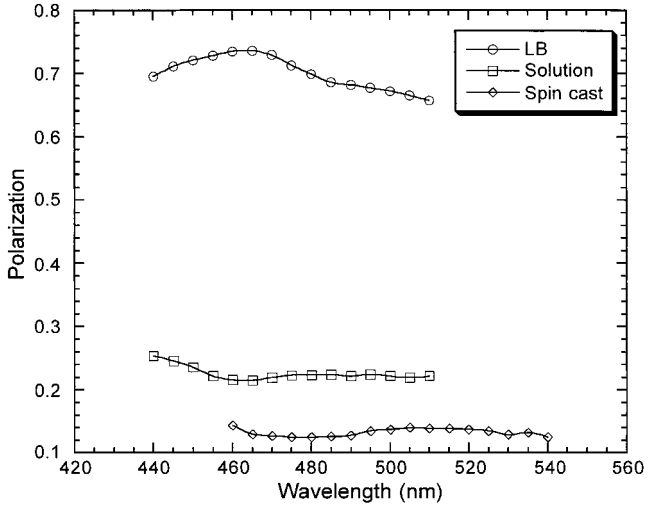

Figure 4. Polarization measurements (λ_{ex} = 420 nm) as a function of wavelength for samples of **1** in different environments.

We likewise have found evidence for energy migration in polarization measurements of **1** in solution, spin-cast films, and LB films. Polymer **1** is a high molecular weight material (M_n = 81 200) and is rotationally static over the emission lifetime of the polymer. The polarization value, P, has been determined from standard equation $P = (I_{||} - GI_{\perp})/(I_{||} + GI_{\perp})$, where $I_{||}$ and $I_{\perp}$ are the intensities of emissions detected parallel and perpendicular to the polarization vector of the incident light and G is an instrumental correction factor. Theoretically, the highest value of P for a randomly oriented isolated fixed chromophore with coincident transition dipoles for the absorption and emission is 0.5. The polarization values as a function of wavelength (Figure 4) show **1** to exhibit a solution polarization of P = 0.22 at λ_{ex} = 458 nm, which suggests that intramolecular energy migration is present. This reduction in P was confirmed to not emanate from rotational dynamics of **1** by examining solid solutions in poly(methyl methacrylate) (PMMA) with relative concentrations (moles of repeat **1** per mole of repeat PMMA) ranging from 10^{-4} to 10^{-2}. In these solid solutions, the polarization was determined to range between 0.25 and 0.27. The static nature of the solid solution indicates that the decrease in polarization is due likely to intramolecular energy migration. Higher concentrations of **1** in PMMA (10^{-1}) and pure spin-cast films of **1** gave lower values of P = 0.18 and P = 0.12, respectively. These results clearly indicate the presence of additional energy migration mechanisms wherein excitations are transferred between polymer chains. The large polarization of the Langmuir−Blodgett films is due to the fact that the chains are highly aligned, and an anisotropic emission (P = 0.7) shown in Figure 5 is observed with the excitation polarized along the chain alignment. The high fluorescence anisotropy ($I_{||}/I_{\perp}$ = 5.5) in these films compares favorably with other systems also prepared by the LB deposition technique,[22] which were found to display a fluorescence anisotropy of $I_{||}/I_{\perp}$ = 3−4.

Emissive trapping sites were deposited selectively on the film's surfaces by dipping Langmuir−Blodgett films into

(21) (a) Ito, S.; Ohmori, S.; Yamamoto, M. *Macromolecules* **1992**, *25*, 185. (b) Ohmori, S.; Ito, S.; Yamamoto, M. *Macromolecules* **1990**, *23*, 4041. (c) Ito, S.; Okubo, H.; Ohmori, S.; Yamamoto, M. *Thin Solid Films* **1989**, *179*, 445.

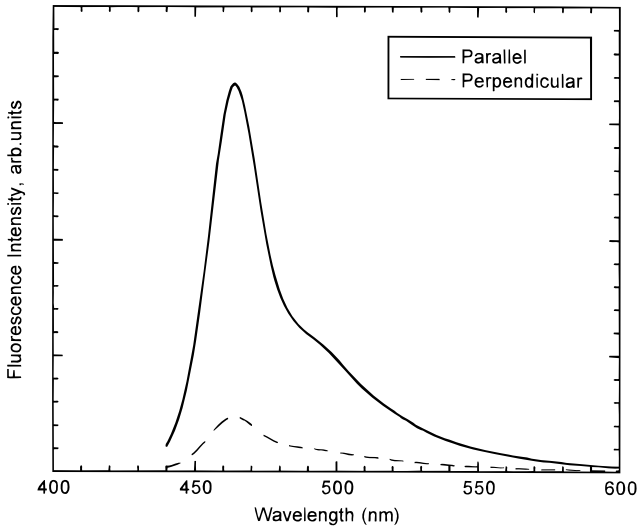

Figure 5. Polarized emission ($\lambda_{ex} = 420$ nm) parallel and perpendicular to the excitation of aligned LB films of **1** with the vector of the excitation light aligned parallel to the polymer's backbone.

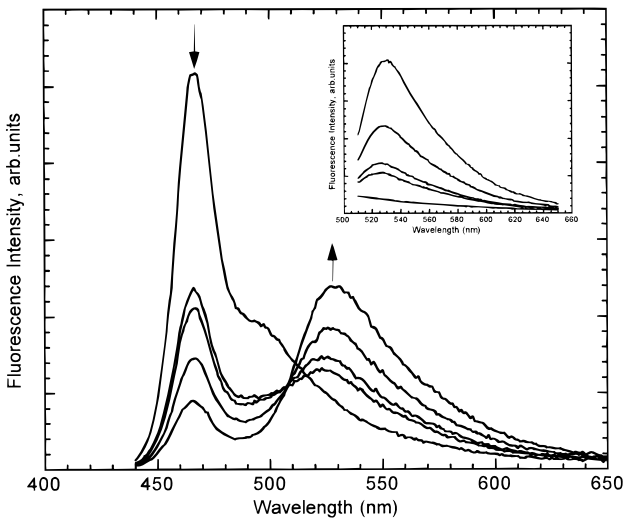

Figure 6. Emission ($\lambda_{ex} = 360$ nm) from a bilayer LB film of **1** treated with increasing concentrations of AO in MeOH before dipping, at 0, 8×10^{-8}, 1×10^{-7}, 3×10^{-7}, and 5×10^{-7} M. The inset shows the emission spectra of the same films when AO was selectively excited at $\lambda_{ex} = 490$ nm. Again the AO emission increases with higher concentrations in the dipping solution, and these data were used to determine the AO concentration.

methanol solutions of Acridine Orange (AO). AO was chosen as the low-energy fluorescent trap because its emission and absorption spectra are well separated from those of **1** and its absorption spectrum has good overlap with **1**'s emission. Additionally, AO exhibits very different solubility, which allows for films of **1** to be dip-coated in solutions of AO with varying concentrations. Irradiation at $\lambda_{ex} = 360$ nm results in selective excitation of the polymer, and any AO emission is the result of energy transfer. Alternatively, AO can be directly excited by irradiation at 490 nm, an energy below the polymer's band gap. Over the concentration ranges examined, the shape and position of the AO emission are practically unchanged (Figure 6, inset). Treatment of films with AO solutions having concentrations $\geq 5 \times 10^{-7}$ M or higher resulted in a red-shifted broadened spectrum indicating the formation of AO aggregates. The onset of this process is observed in Figure 6 with a small red shift at higher AO concentrations. However the monomer emission still dominates, and the quantum yield of AO can be used to measure its relative concentration. It should be noted that our modeling (*vide infra*) only makes use of data from low AO concentrations. Figure 6 shows the emission behavior of a bilayer LB film with varying concentrations of AO deposited on its surface. Clearly, as the AO concentration increases, so too does its fluorescence intensity.

It also is important to note that AO was found to selectively localize at the film's surface. This localization can be deduced from the constant ratio of AO fluorescence intensity between films of different thicknesses examined immediately after dipping or after extended periods of time. Over the time of these investigations, the AO emission intensity decreased, presumably due to sublimation or aggregation, while the polymer emission remained constant. If AO had diffused into the interior of the polymer films, we would expect changes that were a function of the film thickness. The fact that the decrease in AO emission was proportionally the same for different-thickness samples indicates that it does not diffuse into the film. Polarization measurements ($\lambda_{ex} = 490$ nm, $\lambda_{det} = 520$ nm) show the AO transition dipole to be principally aligned parallel to the polymer chain. Excitation parallel and perpendicular to the polymer alignment gave P values for AO of 0.50 and 0.24, respectively.

The rate constants for the energy transfer and decay rates of LB films modified with AO are outlined for a three-layer system in Figure 7. To formulate the necessary analytical equations, we considered a variety of processes including direct energy transfer to the surface trap from different layers, energy transfer between layers, and emission from the polymer and the trap. Poly(phenylene ethynylenes) have a relatively large band gap and a narrow bandwidth,[23] and as a result, the excitations are assumed to exist as strongly bound excitons. Using a steady-state population of all excited species allows the formulation of balanced equations shown in Figure 7. The generalization of these equations to an N-layer system, provides eqs 1 and 2.

$$-n_p^i(k_p + k_{p-t}^i + \sum_{i \neq j}^{N} k_{p-p}^{ij}) + \sum_{i \neq j}^{N} n_p^j k_{p-p}^{ji} + J = 0 \quad (i = 1, 2, ..., N) \quad (1)$$

$$-n_t k_t + \sum_{i=1}^{N} n_p^i k_{p-t}^i = 0 \quad (2)$$

We began our analysis with the simplest situation: a monolayer structure. In accordance with a well-known result,[24] the average lifetime of an excitation (τ) in an infinite one-dimensional chain with randomly distributed efficient quenching traps is $\tau = 1/(2WC^2)$, where C is the trap concentration and W is the hopping rate between neighboring sites. As a result, the steady-state transfer rate, k_{p-t}^1, should be proportional to C^2. In contrast, we find the degree of energy transfer to AO traps, Y_t/Y_p, for a monolayer ($N = 1$) of **1** to have a linear dependence on C, $Y_t/Y_p \sim k_{p-t}^1 \sim C$, where Y_t and Y_p are the emission yields of trap and polymer, respectively (Figure 8). To account for k_{p-t}^1 being proportional to the trap concentration, we must consider that our system provides either one-dimensional energy migration with inefficient trapping or two-dimensional transport.[25,26] We speculate that two-dimensional energy migration

(22) Cimmrová, V.; Remmers, M.; Neher, D.; Wegner, G. *Adv. Mater.* **1996**, *8*, 146.

(23) Brédas, J.-L. In *Handbook of Conducting Polymers*; Skotheim, T. J., Ed.; Dekker: New York, 1986; Chapter 25.

(24) Montroll, E. W. *Phys. Soc. Jpn.* (*Suppl.*) **1969**, *26*, 6.

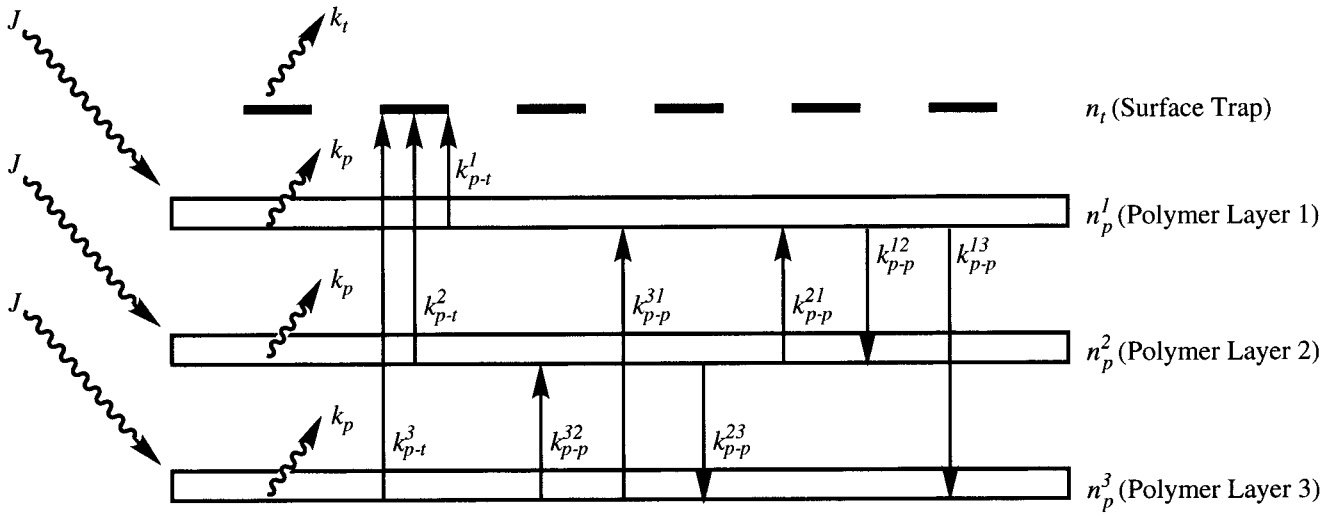

J : Intensity of steady state excitation.

$n_{p,t}$: Excitation population in polymer layers and traps.

$k_{p,t}$: Decay rates of polymer and trap. $k_p = \frac{1}{\tau_p}$, $k_t = \frac{1}{\tau_t}$

k^1_{p-t} : Rate constant for energy migration from polymer layer 1 to the trap. $k^1_{p-t} \sim C$, where C is the concentration of traps.

$k^{2,3}_{p-t}$: Rate constant for direct energy transfer to the trap from polymer layers 2 and 3. $k^2_{p-t} \sim \frac{C}{\ell^6}$, $k^3_{p-t} \sim \frac{C}{(2\ell)^6}$

ℓ is the thickness of layer.

k^{ij}_{p-p} : Rate contant for energy transfer between polymer layers i and j. $k^{ij}_{p-p} \sim \frac{1}{(\ell(i-j))^6}$

A steady state assumption for n_t, n^1_p, n^2_p, and n^3_p gives:

$$-n_t k_t + n^1_p k^1_{p-t} + n^2_p k^2_{p-t} + n^3_p k^3_{p-t} = 0$$

$$-n^1_p k_p - n^1_p k^1_{p-t} - n^1_p k^{12}_{p-p} - n^1_p k^{13}_{p-p} + n^2_p k^{21}_{p-p} + n^3_p k^{31}_{p-p} + J = 0$$

$$-n^2_p k_p - n^2_p k^2_{p-t} - n^2_p k^{21}_{p-p} - n^2_p k^{23}_{p-p} + n^1_p k^{12}_{p-p} + n^3_p k^{32}_{p-p} + J = 0$$

$$-n^3_p k_p - n^3_p k^3_{p-t} - n^3_p k^{32}_{p-p} - n^3_p k^{31}_{p-p} + n^1_p k^{13}_{p-p} + n^2_p k^{23}_{p-p} + J = 0$$

Figure 7. Schematic representation and rate constants for a three-layer LB assembly of polymer with an emissive trap placed at the film surface. The equations resulting from a steady-state excitation population of the layers and the trap are shown.

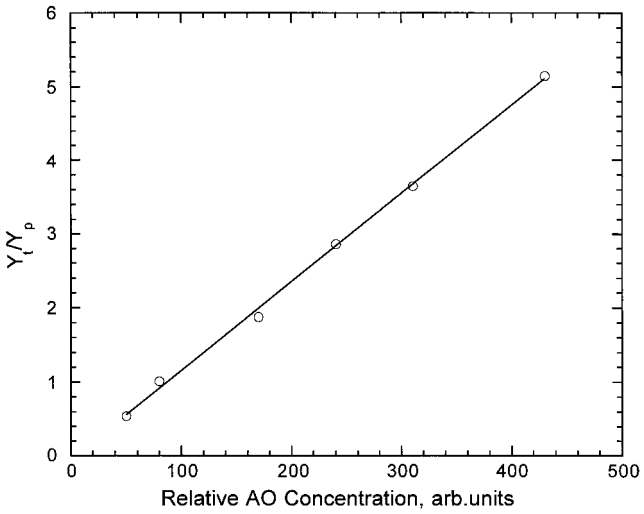

Figure 8. Plot showing the linear dependence of Y_t/Y_p ($\lambda_{ex} = 360$ nm) as a function of AO concentration in a monolayer LB film of **1**.

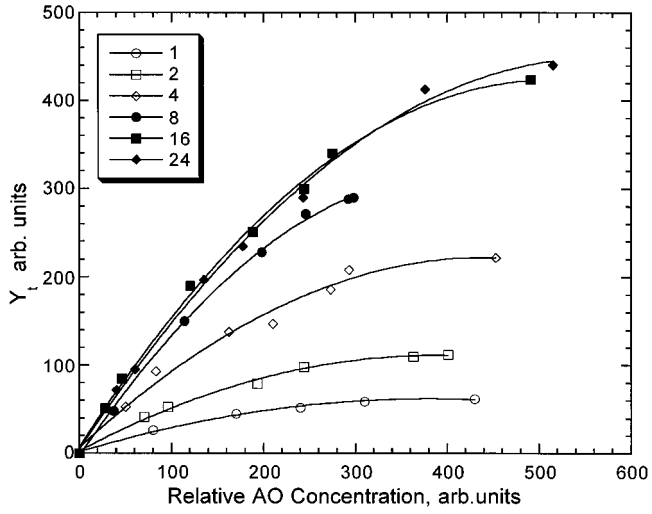

Figure 9. Summary of AO fluorescence ($\lambda_{ex} = 360$ nm, $\lambda_{det} = 525$ nm) obtained from LB films of **1** with different numbers of layers and concentrations of AO.

is most likely, considering that monolayer films of the polymers organize into highly aligned structures, thereby allowing the excitations to undergo efficient interpolymer energy transport.

Figure 9 shows the AO fluorescence intensity plotted against the relative trap concentration for LB films with different numbers of layers. Two key observations can be made from

these curves. Increasing the number of polymer layers increases the AO emission. This increase appears to saturate at approximately 16 layers. We also observe the AO fluorescence to have a linear concentration dependence at low concentrations of the AO trap. Recall that this feature was also observed in the monolayer system. This last point leads us to the conclusion that, at low AO concentration, the steady-state transfer rate in a monolayer film, k^1_{p-t}, is less than $k_p = 1/\tau_p$, where τ_p is the polymer's excitation lifetime. Considering the balanced equations (1) and (2) ($N = 1$), we find that $Y_t \sim k^1_{p-t}/(k^1_{p-t} + k_p)$, and Y_t can only be proportional to k^1_{p-t} if k^1_{p-t} is $< k_p$. The fact that the relative fluorescence of AO, Y_t, increases with increasing numbers of polymer layers is a direct indication of a transition to a three-dimensional energy migration topology. The observation of saturation behavior in films with higher numbers of layers is a manifestation of the diffusion length for energy migration. X-ray measurements performed on the monolayer and multilayer films[17] have shown that the thickness per layer is 11 Å. Since the bimolecular Förster radius for most organic compounds is 20−60 Å, we believe that excitation transfer between polymers must be involved as part of the mechanism for direct energy transfer to the AO trap. This result is also in accord with our polarization measurements.

We can further determine if energy migration in the Z direction (normal to the layer planes) is occurring by using the following argument. If we omit the k^{ij}_{p-p} component, the excitations from a given layer ($i > 1$) will be captured by the surface traps with an energy transfer rate *of* $k^i_{p-t} \sim 1/((i-1)l)^6$, where l is the thickness of one layer and there is exclusively direct energy transfer. We assume the energy migration in a given layer is fast to allow the excitation to arrive within the layer at a point spaced $\approx(i-1)l$ from the AO trap. The latter assumption is obviously a simplification that may contribute in part to deviations between our theory and the observed behavior. An expression for $R(N) = Y_t(N)/Y_t(1) = n_t(N)/n_t(1)$, eq 3, can be

$$R(N) = 1 + \frac{k^1_{p-t} + k_p}{k^1_{p-t}} \sum_{i=2}^{N} \frac{k^i_{p-t}}{k^i_{p-t} + k_p} = 1 + \frac{B(1+A)}{A} \sum_{i=2}^{N} \frac{1}{B + (1-i)^6} \qquad (3)$$

obtained from eqs 1 and 2 with $k^{ij}_{p-p} = 0$. This relationship can be given a functional form where $k^1_{p-t}/k_p = A < 1$ and $k^i_{p-t}/k_p = B/(i-1)^6$ for ($i > 1$). However, in eq 3, $Y_t(N)$ reaches saturation very fast and cannot be fit with our experimental data for any values of A and B. As a result, we can conclude that direct energy transfer, as the only mechanism for delivery of energy to the AO trapping sites, is inconsistent with our experimental results.

Taking into account that there must be energy migration in the Z direction (k^{ij}_{p-p} is finite) leads to eq 4, where n^i_p is a

$$R(N) = 1 + \frac{1+A}{A} \sum_{i=2}^{N} k^i_{p-t} n^i_p \qquad (4)$$

solution of eqs 1 and 2 depending upon the parameters $k^1_{p-t}/k_p = A < 1$, $k^i_{p-t}/k_p = B/(i-1)^6$, and $k^{ij}_{p-p}/k_p = D/(i-j)^6$. Recall that we had earlier shown that $k_p > k^1_{p-t}$. The parameters B and D characterize the direct energy transfer to the surface trap from layer i and the energy transfer between layers i and j, respectively. The best fit for the experimental data obtained by a numerical solution of eq 4 gives the following: $D \geq 10^2$, $A/B = 0.5$, and $A = 0.8-0.2$.

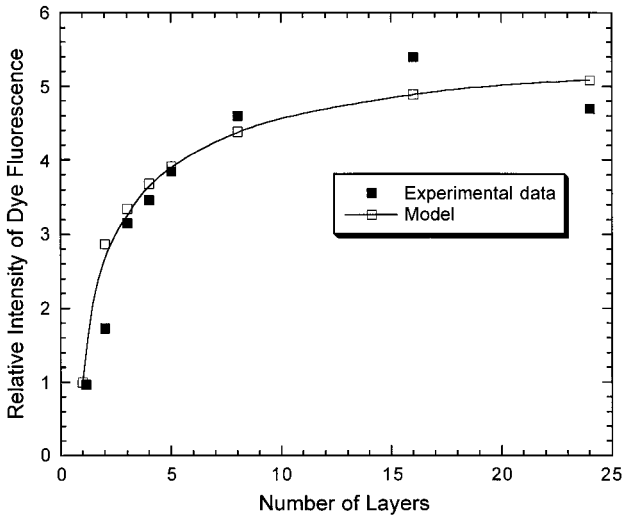

Figure 10. AO fluorescence Y_t (normalized to that obtained for a single monolayer) as a function of the number of LB layers. The experimental points were as the slope of the linear region of the plot shown in Figure 9. The plot shows the best fit of the experimental data by the modeling procedure (eq 4).

The correlation between experimental data and the model values is shown in Figure 10. The value D defines a ratio of the transfer rate between nearest neighbor layers and the polymer's radiative rate, and D's magnitude indicates that there is fast energy migration between polymer layers. Substituting the radiative rate of the polymer into the relationship indicates that $k^{i,i-1}_{p-p} \geq 6 \times 10^{11}\ s^{-1}$. This value is consistent with typical Förster energy transfer rates in organic solids.[27] Additionally, because we have fast excitation exchange between different layers ($k^{i,i-1}_{p-p} \gg k^i_{p-t}$), we can approximate that the excitation populations are equal in all layers. As a result, $Y_t(N)$ will depend on $n_p \sum_{i=1}^{N} k^i_{p-t}$ in accord with eq 2. If we were to again consider that $k^{ij}_{p-p} = 0$, then the populations will be different in each layer and $Y_t(N)$ would reach saturation much faster. Since our results indicate fast interlayer energy transport, the $Y_t(N)$ dependence upon film thickness should be greater than would be expected from the Förster radius.

Considering the excitation lifetime and the rate of energy transfer between layers, we find that the number of excitation hops, S, in the Z direction is in excess of 100 (for simplicity we have considered only hops between nearest neighbor layers). This result yields a mean-squared displacement, or diffusion length, which is $> lS^{1/2}$, or about the thickness of about 10 layers.

There are a number of limitations to our model and solutions which should be noted. Our fitting procedure requires A and B to be dependent parameters. This condition is justified by the fact that at low concentrations k^1_{p-t} and k^i_{p-t} ($i > 1$) are proportional to the AO concentration. Using this restriction, we find that the ratio of $A/B = 0.5$ maintains a satisfactory fit over the range given, and for values of $A < 0.2$ the fit becomes noticeably worse. Our model does not explicitly describe the intralayer energy transport, and we have used the fact that

(25) Onipko, A. I.; Malysheva, L. I.; Zozulenko, I. V. *Chem. Phys.* **1988**, *121*, 99.

(26) Kenkre, V. M. In *Exciton Dynamics in Molecular Crystals and Aggregates*; Hohler, G., Ed.; Springer: Berlin, 1982.

(27) Pope, N.; Swemberg, C. E. *Electronic Processes in Organic Crystals*; Oxford University Press: New York, 1982.

intramolecular transport should result in fast intralayer transport relative to interlayer transport. This results in an assumption that the excitation can arrive at a distance of $\approx(i-1)l$ from the trap. However, if there is a contribution from long-range transfer to the traps combined with energy migration,[28] a deviation from the $1/(i-1)^6$ distance dependence used in our model would be expected. Perhaps a more significant limitation is the fact that our model does not take into account the energetic disorder due to statistical distribution of conjugation lengths.[7] However, in these systems, the hopping rate is asymmetric between sites of different energies and the excitations preferentially migrate to sites with a lower energy. To our knowledge, the effect of energetic disorder on the steady-state transport properties of systems in restricted geometry (Z in our case), which is distinct from transport in one- and three-dimensional systems studied with pulsed excitation,[7,29] is unknown.

Conclusion

The energy migration in anisotropic multilayer assemblies of polymer **1** display rapid intralayer as well as interlayer energy transport. Transport between polymer molecules and layers in these systems is dominated by dipole−dipole mechanisms which are facilitated by the alignment of the molecules. The increase in the efficiency of energy migration to the surface traps (larger AO emission, Y_t) with increasing film thickness may, at first glance, seem counterintuitive since the relative AO concentration relative to that of the polymer is actually smaller in thicker films. However, this increased trapping efficiency is direct manifestation of the transition to a three-dimensional behavior that necessarily creates a more efficient trapping process. The modeling has determined that the rate of energy transfer between layers exceeds 6×10^{11} s^{-1}. This high rate results in a uniform excitation population throughout all the layers of the films. The results of these studies are of interest for the design of more efficient fluorescent-based sensors. It is clear from these studies that an optimal thickness will exist in sensor schemes requiring trapping at the polymer surface. Additional enhancements in the energy migration may be possible by creating multilayer structures which provide vectorial energy transport in a specific direction. This effect can be accomplished by using a ladder of band gaps to direct the excitations to hopping sites in the polymer films.

(28) (a) Klein, U. K. A.; Frey, R.; Hauser, M.; Gösele, U. *Chem. Phys. Lett.* **1976**, *41*, 139. (b) Gösele, U.; Klein, U. K. A.; Frey, R.; Hauser, M. *Chem. Phys. Lett.*, **1975**, *34*, 519.

(29) Levitsky, I. A. *Phys. Rev. B* **1994**, *49*, 15594.

Experimental Section

All solution measurements and spin-casting were performed using spectroscopic grade chloroform. A detailed investigation of the Langmuir−Blodgett deposition of **1** and the film thickness is described elsewhere.[17] Films were deposited on hydrophobic substrates. Acridine Orange (AO) was obtained from Aldrich Chemical Co. and used without purification. The AO-modified LB films were prepared by dipping films into solutions of methanol solutions of the dye at concentrations varying from 5×10^{-8} to 7×10^{-7} M for 20 s followed by drying. Solution measurements utilized concentrations of 7×10^{-6} M of repeat **1**. Spin-cast films were prepared on quartz substrates with a spinning rate of 3000 rpm. UV−vis spectra were obtained from a Hewlett-Packard 8452A diode array spectrophotometer. Fluorescence studies were conducted with a SPEX Fluorolog-τ2 fluorometer (model FL112, 450 W xenon lamp) equipped with a model 1935B polarization kit. Polymer thin-film spectra were recorded by front-face (22.5°) detection. All emission and excitation spectra were corrected for the detector response and the lamp output. The time of fluorescence decay was determined by a phase-modulation method using frequencies from 10 to 250 MHz and using glucose−water solutions (scattering sample, $\tau = 0$, right-angle geometry) and methanol solutions of *p*-bis[2-(5-phenyloxazolyl)]-benzene (fluorescence, $\tau = 1.46$ ns, front-face geometry) as standards. The same polymer solution lifetimes (±5%) were obtained using these standards for both front-face and right-angle geometries. The experimental errors were typically 2−4% in the phase angle at lower frequencies and somewhat higher (5−8%) above 200 MHz. The phase modulation curves were fit with the GLOBAL analysis program (University of Illinois) and software developed in-house. The numerical solutions were obtained using the NAG program which was developed in part by I.A.L. at the Ukraine Academy of Sciences; however, the same solutions may be obtained by any mathematical program capable of solving a series of linear equations.

Acknowledgment. The authors gratefully acknowledge funding from the Office of Naval Research and the Defense Advanced Research Projects Agency.

JA982610T